UNIVERSITY of CALIFORNIA
SANTA CRUZ

THE HIDDEN FRIEND'S WAKE: DARK MATTER AND A BINARY AT THE GALACTIC CENTER

A thesis submitted in partial satisfaction of the
requirements for the degree of

BACHELOR OF SCIENCE

in

ASTROPHYSICS

by

Samuel D. English

12 June 2022

The thesis of Samuel D. English is approved by:

Professor Stefano Profumo
Advisor

Professor Bruce A Schumm
Chair, Department of Physics

Abstract

The Hidden Friend's Wake: Dark Matter and a Binary at the Galactic Center

by

Samuel D. English

Recent dynamical evidence suggests that Sgr A*, the massive object at the center of the Milky Way, may be a binary of two black holes rather than a single black hole. The existence of such a binary has dynamical consequences for the distribution of dark matter at the galactic center, with dramatic implications for dark matter annihilation signals. We show that the existence of a binary companion would significantly relax constraints on the dark matter annihilation cross section from the galactic center, and would substantially weaken the case for dark matter annihilation as the origin of the claimed galactic center excess. By relaxing these constraints with the consideration of a companion black hole, we completely open up the door to previously eliminated bands of dark matter candidates, revitalizing our search focus and providing further fodder for future dark matter exploration.

Contents

Figures

Tables

To my cat,

Momo,

for always keeping me company.

Acknowledgements

I would like to recognize the impact the Ron Ruby Undergraduate Research Award and Koret Undergraduate Research Scholarship had on conducting meaningful research in collaboration with Benjamin Lehmann and Stefano Profumo. Thanks to their aid, I was able to give an oral presentation at APS 2022 New York and later craft a poster to interact with the undergraduate body at UCSC through the Koret Scholar Slam event. With gifted funding providing me proper academic resources, with empathetic leadership from Ben, with expert guidance and wisdom from Stefano, with everyone's understanding and encouragement, my family, partner, and friends included, I have been able to do what I love most.

1

Introduction

Let us now embark on a journey, a journey from Earth to a galaxy not so far away. Our story begins at the heart of our very own. Between the thousands of millions of stars speckled across our Milky Way galaxy, we come to Sagittarius A* (Sgr A*), a supermassive black hole (BH) resting directly at its center.

Now, luminous matter tends to agglomerate towards this insanely dense object, but as does particulate dark matter (DM). Thus, BHs are thought to aid the formation of DM density spikes, which, conveniently, provide a fantastic spot to look for DM annihilation signatures! In turn, one can set constraints on features of the DM such as the annihilation rate. Specifically, for any given theory of weakly-interacting DM or WIMP[i], one may expect to have particle collisions and decays which produce

[i] Weakly Interacting Massive Particle (WIMP), a common framework for theories of dark matter.

some cascade of Standard Model particles[ii]. This production of new entities have many possible outcomes or channels through which the resulting constituent parts would be detectable by our instruments on Earth. If we can detect an excess of annihilation signals related to a given DM theory, then bingo! We've got ourselves a sure-fire method of statistically detecting the presence of DM particles and relevant parameters which can allude to the deeper nature of DM.

Galactic nuclei, in general, represent a uniquely rich physical space in which dynamic processes occur and the greatest density of DM exists. As a natural stage for the study of these topics, the center of our Milky Way has been subject to intense exploration: authors have studied the behavior of DM near the galactic center [1], the central BH, Sgr A* [2], as well as the formational history of the galaxy [3]. The former has been a topic of immense intrigue in light of the ongoing galactic center excess problem: the outstanding bump in GeV emissions from the Milky Way's galactic center region could be accounted for by suspected DM annihilation [4].

1.1 Our Hidden Friend

As it turns out, these density spikes may not be stable to the perturbations they encounter over their lifetimes [5], one such perturbation being the presence of a binary

[ii] As opposed to some Dark Sector particles, which cannot be directly observed to interact with our detectors.

companion to the central BH. The presence of adiabatic[iii] spikes hinges on a plethora of deeply bound cold orbits to the BH [6]. Any sort of disturbance such as a merger [7], scattering from stars [8], or an off-center seedling BH [1] can kick out these particles and prevent spike formation. As we soon discover, this would cause signals from DM annihilation (or decay) to be, unexpectedly, much fainter than previously thought.

In fact, one can easily think of a case in which Sgr A* is not alone: to support this theory, let us first consider the formational history of galaxies.

Over billions of years, galaxies (on average) tend to collide, consolidating the entirety of their physical contents [3]. Furthermore, we now know that almost all galaxies contain a seedling BH at their center [9]. Thus, let's put two and two together and imagine a reality in which the closest such system, our Milky Way, has combined with another galactic entity in its recent cosmological past [10] [11].

In this scenario, our supermassive BH Sgr A* could still be in the process of merging with another BH. Although, this type of configuration is constrained by observation: make the companion BH too weak of an influence or too massive and we directly conflict with stability constraints [12].

There is hope yet: we still have a large swathe of parameter space in which this reality can exist (Fig. 2.2). With new scientific instruments[iv] prepared to come online

[iii] Energy neither enters nor leaves the system.

[iv] EHT, the future LISA gravitational-wave mission, for example.

soon, this is precisely the time for theorists to pose the question and inquire: what *if* a companion BH to Sgr A* exists in our Milky Way?

Well, our "hidden friend" [12], if there, will vastly influence the surrounding, local DM distribution, and luminosity of DM self-annihilation. This has significant implications as to the pertinence of certain DM models in our hunt for DM.

1.2 Asking the Question

1.2.1 Spike at the Center of our Milky Way?

The cuspy halo problem (core-cusp problem) deals with the discrepancy between DM density profiles predicted by cosmological N-body simulations and actual observations taken from low-mass galaxies. While simulations tell us that DM density should increase steeply as we approach very small radii, the rotation curves of observed dwarf galaxies illustrate a different story: rather, density profiles should have a flat, central DM "core."

This core-cusp problem has yet to be resolved. However, it has been recognized that, with an absence of baryons in simulation, one will then find cuspy (singular) DM density profiles toward galactic centers [13]. Inclusion of such baryonic feedback effects helps skew the debate towards cored (flatter) distributions [14]. Furthermore, there are many cases in which weakly-interacting DM can feasibly yield an, altogether, better fit for a wide range of galactic structures [15]. Here, we attempt to reconcile this issue with a generic WIMP candidate, showing that cuspy, simulation spikes are

unphysical due to a variety of potential physical perturbations. Here we re-introduce our nuclear relic of some smaller galaxy that once merged with the Milky Way [12].

How would a companion BH affect the potentially weakly-interacting, DM density spike[v] in our own galaxy? To understand this, we must also understand the case of a single BH in the presence of a DM halo.

In this thesis, we study the dynamical effects of a binary to Sgr A* in our Milky Way's galactic center, focusing on the unconstrained parameter space for a companion. We show that, if such a binary is discovered e.g. the Event Horizon Telescope, there will be immediate implications for DM annihilation bounds and the significance of DM in our interpretation of the galactic center excess.

Let's first assume ideal conditions to help simplify the mathematical rigor and build our intuition to the case we wish to, ultimately, solve.

[v] Assuming a spike has formed in the past, we ask what a companion would do to it.

2

Previous Work

2.1 Single BH

A sharp, DM density spike forms at the center of our own galaxy. In the absence of baryonic matter and other external entities, the only other object here is a single, central BH: Sgr A*.

2.1.1 Density Spike Formation

Looking to the literature, we find that authors Gondolo & Silk [16] have done a very thorough analysis of capturing the DM density profile's response to the presence of a BH, in isolation.

We consider a generic, cuspy power law profile with some slope parameter, γ, which informs the "steepness" of the density spike, alongside normalization constants r_0 and ρ_0 (scale radius and density):

$$\rho(r) = \rho_0 \left(\frac{r}{r_0}\right)^{-\gamma}, \quad 0 < \gamma < 2. \tag{2.1}$$

After planting our seedling BH as astrophysical farmers, we patiently wait for it to adiabatically grow until our system is in equilibrium. Thereafter, we ask: what does the density profile *after* BH formation look like? Realistically, one performs an action integral[i] and determines the final density after BH formation from the final phase-space distribution [16].

We end up with a very similar picture: a modified power law with a new, evolved slope parameter and normalization constants,

$$\rho'(r) = \rho_{\rm R}\ g_\gamma(r) \left(\frac{R_{\rm sp}}{r}\right)^{\gamma_{\rm sp}}, \quad 2.25 < \gamma_{\rm sp} < 2.5. \tag{2.2}$$

Look! With the addition of a single BH to our DM halo, we see that the density profile strictly increases in steepness.

Using a very powerful physics tool called scaling arguments, we discover that the

[i] In the field of the power-law profile, with potential proportional to $r^{2-\gamma}$, one must find an approximation over all phase space since the action integral cannot be performed numerically [16].

new slope parameter $\gamma_{\rm sp}$ goes as

$$\gamma_{\rm sp} = \frac{(9-2\gamma)}{(4-\gamma)}. \tag{2.3}$$

Our new scale density constant, $\rho_{\rm R}$ looks like

$$\rho_{\rm R} = \rho_0 \left(\frac{R_{\rm sp}}{r_0}\right)^{-\gamma}, \tag{2.4}$$

which naturally leads us to define the new scale radius, $R_{\rm sp}$:

$$R_{\rm sp} = \alpha_\gamma r_0 \left(\frac{M}{\rho_0 r_0^3}\right)^{1/(3-\gamma)}. \tag{2.5}$$

A quick clarification: m_1 here represents the mass of the central BH, Sgr A*. Previous groups have estimated the mass to be $m_1 = (2.6 \pm 0.2) \times {\rm M}_\odot$ (*not* equivalent to M in other mentions of mass variables) [2].

Crucially, we have yet to establish what $g_\gamma(r)$ and α_γ represent. Unfortunately, both of these variables cannot be obtained analytically. Rather, we must employ numerical techniques to grasp, and possibly approximate their form.

First, the authors from [16] illuminate this discussion in finding that $g_\gamma(r) \approx (1 - 4R_{\rm S}/r)^3$, the factor accounting for particle capture over our defined range of γ. Crucially, this implies that $g_\gamma(r)$ will only significantly contribute when $R_{\rm S}$, the Schwarzschild radius associated with the central BH, is much greater than some radius r of interest ($r << R_{\rm S}$). Otherwise, $g_\gamma(r) \to 1$. The fact that Sgr A*'s Schwarzschild

radius is on the order of 10^{-1} au directly implies that this factor is insignificant for our radii of interest (of $\mathcal{O}(1)$).

Last, we must understand the normalization factor α_γ. The paper [16] also provides the following values:

γ	α_γ
0.05	0.00733
0.2	0.120
0.4	0.140
0.6	0.142
0.8	0.135
1.0	0.122
1.2	0.103
1.4	0.0818
2.0	0.0177

Table 2.1: Numerically obtained values [16] for normalization parameter $\alpha_\gamma(\gamma)$, used in calculation of R_{sp}, embedded within density profile $\rho'(r)$.

With the aid of Mathematica, we perform a simple interpolation of this well-behaved set of data points. This allows us to easily calculate α_γ for any given input value of the slope parameter γ as we explore different physical scenarios.

2.1.2 DM Self-Annihilation

Considering any generic model of weakly-interacting, massive particles (WIMP) as a candidate for the DM contents of our universe, one must account for self-

interactions in the form of collisions, annihilation events, and decays. Crucially, DM self-annihilation will deplete a portion of the inner regions of our DM halo. So, despite any increase in density towards the center of our system due to the BH's presence, there will be some maximal DM density, $\rho_{\rm core}$, at which annihilation effects will prevent *any* further accumulation of DM particles [16]:

$$\rho_{\rm core} = \frac{m}{\sigma v \cdot t_{\rm BH}}. \tag{2.6}$$

Specifically, we see that our maximal or critical density for annihilation depends on the mass of our DM particle candidate (m), its annihilation cross section times its relative velocity (σv), as well as the age of the BH itself ($t_{\rm BH}$), which we conservatively set to the scale of gigayears. This comes with an associated cutoff radius, $R_{\rm core}$, below which we expect to see a constant density profile set by $\rho_{\rm core}$:

$$R_{\rm core} = R_{\rm sp}\left(\frac{\rho_{\rm R}}{\rho_{\rm core}}\right)^{\frac{1}{\gamma_{\rm sp}}}. \tag{2.7}$$

This set of equations to calculate the critical density associated with DM self-annihilation is, in fact, generic for any given WIMP DM model of our choosing!

Let's combine both the evolved DM halo in the presence of a BH with our annihilation effects (Eq. (2.6), Eq. (2.2)) in the following way:

$$\rho_{\rm sp}(r) = \frac{\rho'(r)\rho_{\rm core}}{\rho'(r) + \rho_{\rm core}}. \tag{2.8}$$

We amalgamate ρ' and $\rho_{\rm core}$ to obtain $\rho_{\rm sp}$, which will represent the complete DM density profile for our simplified, single BH surrounded by a DM halo. A great way to reinforce our understanding of this situation is to look at some plots:

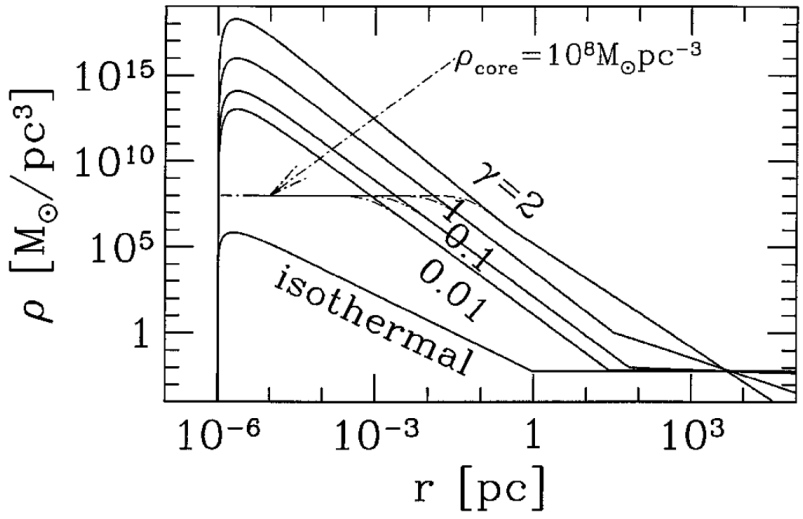

Figure 2.1: Multiple examples of density spike profiles [16], with illustration of annihilation-caused coring radius (taken from Fig. 1 of [16]).

Fig. 2.1 depicts density as a function of radius for various density profiles with different values of gamma, our slope parameter. Most importantly for us to take away from this, is the cutoff at which $\rho_{\rm core}$ sets the maximal density for the interior region of our system. Now, let's introduce our hidden friend.

2.2 Sgr A* Hidden Friend Constraints

Quickly, before we do any intensive math, let's recall why we're thinking about this scenario in the first place. The hierarchical nature of galaxy formation suggests that a supermassive BH binary could exist in our GC (Sec. 1.2.1). In addition, we have upcoming tools and proposals to further constrain possible orbital configurations of such a binary companion to Sgr A* through measurements of stellar orbits, for instance [12].

Smadar Naoz et al. (2019) recently published a paper placing bounds on orbital stability of a binary companion, narrowing its possible configurations in phase space [12]. We see for a wide range of the companion's mass on the x-axis and initial binary separation on the y-axis, such a system could, in fact, exist in our Milky Way in the so-called "allowable regime" (Fig. 2.2).

Naoz et al. argues that precise measurements of the time variability of orbital parameters for other stars will allow further narrowing of the potentially allowable scenarios.

2.3 Binary BH System

As it turns out, a DM overdensity significantly alters the dynamics of the kinds of BH merger systems we wish to explore.

Consider a BH merger with some surrounding dress of DM. Kavanagh, et al. shows that a fixed DM dress is unphysical for a range of binaries and DM distributions [17].

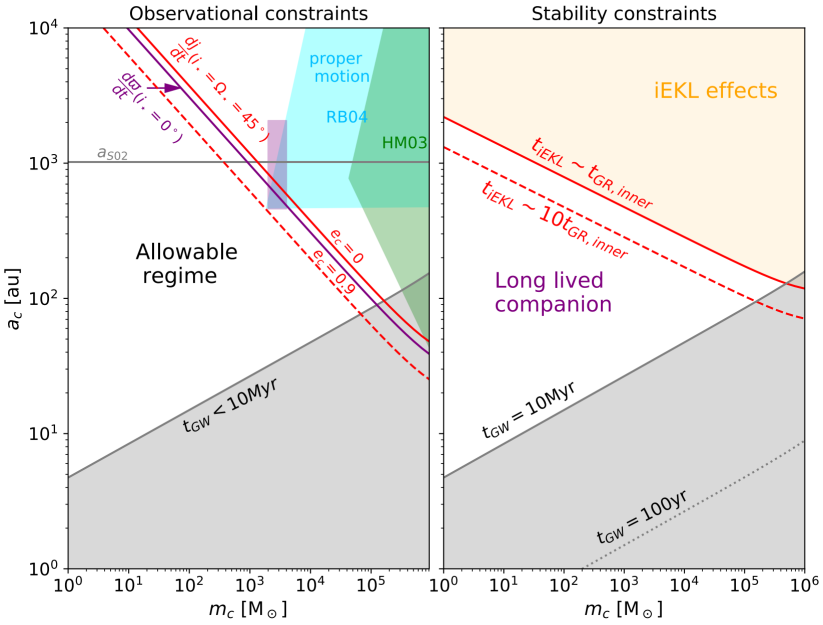

Figure 2.2: Constraints on the mass-semimajor axis parameter space of a hypothetical companion to Sgr A*. Of primary interest is the left hand side plot which illustrates, for the most current, stringent constraints, what swathe of parameter space ("allowable regime") a companion BH could physically exist in (taken from Fig. 3 of [12]).

So, instead, we must think of a formalism to self-consistently follow the evolution of our DM dress due to its gravitational interaction with the binary.

The presence of DM exerts a dynamical friction force on the compact object, causing it to fall more quickly towards the central BH. In astrophysics, dynamical friction is also referred to as gravitational drag, representing the loss of kinetic energy and momentum of a moving body through gravitational interactions with surrounding matter in space. In this adiabatic process, energy conservation is satisfied in that the orbital energy change with time is equal to the power radiated by gravitational waves along with the power associated with dynamical friction losses,

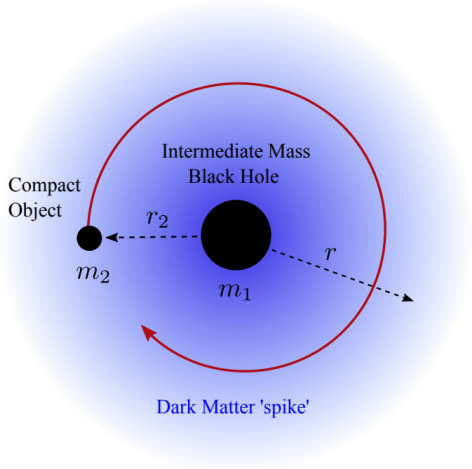

Figure 2.3: Intermediate mass-ratio inspiral (IMRI) system surrounded by a DM dress [17]. A central BH of intermediate mass m_1 is in the process of merging with a compact object ($m_2 < m_1$) at some orbital radius, r_2. The system is further encased by a dense region of DM particles with an associated density profile, $\rho_{\rm DM}(r)$ (taken from Fig. 1 of [17]).

$$\frac{\mathrm{d}E_{\rm orb}}{\mathrm{d}t} = -\frac{\mathrm{d}E_{\rm GW}}{\mathrm{d}t} - \frac{\mathrm{d}E_{\rm DF}}{\mathrm{d}t}. \tag{2.9}$$

Point being, the energy lost by the compact object is injected into the surrounding DM! This causes an effective expansion of the halo, *further* coring the inner density profile.

For completeness, we define the power of gravitational wave losses (for circular orbits in the quadrupole approximation [17]) as

$$\frac{\mathrm{d}E_{\rm GW}}{\mathrm{d}t} = \frac{32G^4M(m_1m_2)^2}{5(cr_2)^5}, \tag{2.10}$$

where G is the infamous Newton's constant ($G \approx 6.67 \times 10^{-11}$ N·m^2/kg^2), M is the total BH mass ($M = m_1 + m_2$), c is the speed of light ($c \approx 3 \times 10^8$ m/s), and r_2 represents the binary separation[ii]. Specifically, m_1 will be illustrative of Sgr A*'s mass, while m_2 will save the mass of our companion, or hidden friend, BH.

Likewise, dynamical friction losses are given by

$$\frac{\mathrm{d}E_{\mathrm{DF}}}{\mathrm{d}t} = 4\pi(Gm_2)^2\rho_{\mathrm{DM}}(r_2)\xi(v)v^{-1}\log\Lambda, \tag{2.11}$$

where $\xi(v)$ is an $\mathcal{O}(1)$ term which denotes the fraction of DM particles moving slower than the orbital speed [17] (negligible), and ρ_{DM}, the density profile which our binary system is encased within. It is convenient to express these power losses as functions of circular r_2 orbits by utilizing the relationship, $v = \sqrt{GM/r_2}$.

As per argument of Kavanagh, et al. [17], we let the usual Coulomb logarithm become $\log\Lambda = \sqrt{m_1/m_2}$, since the central intermediate mass BH (IMBH) will dominate any contributions to the DM particle dynamics.

[ii] Distance from Sgr A* to the companion BH.

3

Analytic Solution

Simulating everything in detail would be intractable, so we will walk through our simplifying assumptions and procedure to obtain results.

First, we assume that the time evolution of the binary separation, r_2, is negligible on our timescales of interest[i].

More importantly, our second, and biggest assumption, is about the response of the halo to the injected energy. This is in general very hard to calculate, and, right now, we're making the simplistic assumption that the center of the halo completely hollows out. This is certainly wrong to some degree, although, justifiable if one assumes that the halo responds quickly compared to the injected energy—that way, the newly accelerated DM particles have time to move around and find a new equilibrium,

[i] We're also currently looking into allowing it to vary in our differential equations, see Sec. 3.2.

which will have less density in the center.

Now we must track the additional gravitational effects of the binary. The scouring radius, or coring radius due to dynamical friction[ii], is obtained by equating the binding energy of the DM halo to the change in energy of the binary system,

$$r_{\rm sc} \rightarrow E_{\rm BE}(r^*) = \Delta E(r^*). \tag{3.1}$$

This scouring radius will compete with our annihilation coring radius, forcing some maximal density depending on our combination of initial parameters. Simply combining the $\rho_{\rm sp}$ profile we have with this effect, creating a piecewise function that will cut off the density below $r_{\rm sc}$ is sufficient:

$$\rho_{\rm mod}(r) = \begin{cases} 0 & r \leq r_{\rm sc}, \\ \rho_{\rm sp}(r) & r > r_{\rm sc}. \end{cases} \tag{3.2}$$

Now, using both aforementioned assumptions, let's create a central DM spike and place our two BHs into the mixture!

[ii] As described in Sec. 2.3, from [17].

3.1 Static & Spike Solution

3.1.1 G&S Broken Power Law

In order to learn anything about our system or how the dynamics of a companion BH to Sgr A* directly impact the surrounding DM particles, we must understand what that final density profile looks like. Having gone through the exercise of outlining each effect we expect to incorporate, we may, explicitly, show that Eq. (2.8) boils down to

$$\begin{aligned}\rho_{\rm sp}(r) &= \frac{\rho'(r)\rho_{\rm core}}{\rho'(r)+\rho_{\rm core}} \\ &= \frac{\rho_{\rm R}\left(\frac{R_{\rm sp}}{r}\right)^{\gamma_{\rm sp}}\cdot\rho_{\rm core}}{\rho_{\rm R}\left(\frac{R_{\rm sp}}{r}\right)^{\gamma_{\rm sp}}+\rho_{\rm core}}.\end{aligned} \tag{3.3}$$

where $\rho_{\rm R}$ is defined by Eq. (2.4), $\rho_{\rm core}$ by Eq. (2.6), $\gamma_{\rm sp}$ by Eq. (2.3), and $R_{\rm sp}$ by Eq. (2.5). Note that the factor $g_\gamma(r)$ is negligible for us, and the normalization factor α_γ is given by the entries of Tab. 2.1.

With this combination of evolved power law and annihilation coring radius, we now have the backbone of our modified profile which will be defined by Eq. (3.3) above. However, in order for this calculation and the subsequent density profile $\rho_{\rm mod}$ to make sense, we must also discover what our scouring radius is mathematically represented by.

3.1.2 Binding Energy

As seen in Eq. (3.1), the scouring radius we wish to obtain is dependent on both the binding energy and the change in energy of our gravitational system[iii]. Thus, if we hope to comprehend how dynamical friction effects, arising from the companion's presence, will further alter our picture of the GC density profile, we need to get a proper handle on the binding energy of our system. In the case that dynamical friction losses are comparable to the binding energy of our system itself, the inner regions of our DM halo will drastically change, lending to greater and greater values for $r_{\rm sc}$.

Let us ask: what is the binding energy within a given radius for a system comprised of a DM halo surrounding a BH? Here, there are only two components: the self-energy of the cloud and the binding energy to the BH. One may neglect the presence of the companion BH due to it's relatively small mass contribution:

$$U(r<R) = -\underbrace{\int_{r<R} \frac{G\mathrm{d}m_1\mathrm{d}m_2}{r_{12}}}_{\text{DM Cloud}} - \underbrace{\int_{r<R} \frac{Gm_1\mathrm{d}m}{r}}_{\text{Central BH}}. \tag{3.4}$$

[iii] Gravitational waves are negligible in comparison to dynamical friction in this paper's cases of interest based on timescales and binary separation.

Building up the first with shells, we see that

$$-\int_{r<R}\frac{G\mathrm{d}m_1\mathrm{d}m_2}{r_{12}}=-\int_{r'<R}\frac{GM(r<r')\mathrm{d}m}{r'} \tag{3.5}$$

$$=-\int_0^R\frac{G\left(\int_0^{r'}\rho(r)4\pi r^2\mathrm{d}r\right)\rho(r')4\pi r'^2}{r'}\mathrm{d}r'. \tag{3.6}$$

Thus, we write

$$U(r<R)=-\int_0^R\frac{G\left(\int_0^{r'}\rho_{\mathrm{sp}}(r)4\pi r^2\mathrm{d}r\right)\rho(r')4\pi r'^2}{r'}\mathrm{d}r'-\int_0^R\frac{Gm_1\rho_{\mathrm{sp}}(r)4\pi r^2}{r}\mathrm{d}r. \tag{3.7}$$

Because $\rho_{\mathrm{sp}}(r)$'s density profile contains ρ_{core}, which will set the inner annihilation zone, we can just as easily convert this into a simpler density profile, neglected below the associated coring radius.

For example, in evaluating the second integral in Eq. (3.7) containing factors of $\rho_{\mathrm{sp}}(r)$ in our system's potential energy, we show:

$$\begin{aligned}Gm_1\int_0^R\frac{\rho_{\mathrm{sp}}(r)4\pi r^2}{r}\mathrm{d}r\approx\int_0^{r_{\mathrm{out}}}\left(\rho_{\mathrm{sp}}(r)\right)4\pi r\mathrm{d}r&=\int_0^{r_{\mathrm{out}}}\left(\frac{\rho'(r)\rho_{\mathrm{core}}}{\rho'(r)+\rho_{\mathrm{core}}}\right)4\pi r\mathrm{d}r\\&=\int_{r_{\mathrm{core}}}^{r_{\mathrm{out}}}\left(\rho'(r)\right)4\pi r\mathrm{d}r.\end{aligned} \tag{3.8}$$

Assuming $\rho_{\mathrm{core}}>0$, $\rho_{\mathrm{R}}>0$, $r>0$, $r_{\mathrm{sp}}>0$, and $0<r_{\mathrm{core}}<R$ we're able to integrate each potential term. After explicitly calculating the binding energy values

for a generic "Hidden Friend" scenario[iv], we see that the first integral term is negligible in its energy contribution (Fig. 3.1).

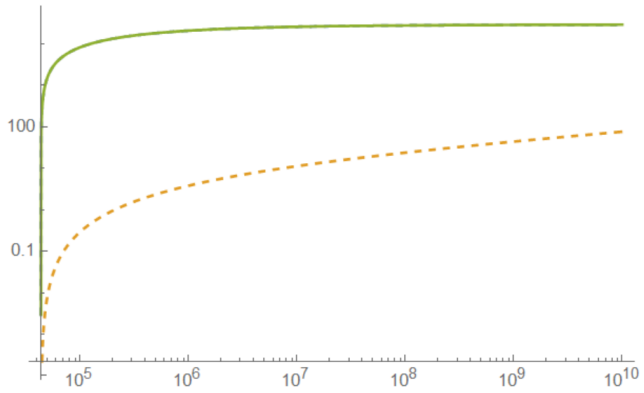

Figure 3.1: Numerical plot of contributive integral terms in Eq. (3.7) (arbitrary units for magnitude of binding energy vs. radius). The green, solid line represents the total binding energy, whereas the lower, golden, dashed line shows the second binding energy term's magnitude (DM cloud's self-binding energy). The first integral term's dashed contribution (binding potential of central BH to DM cloud) is directly on top of the total, implying that the second term is negligible.

Physically, this implies that the self-binding energy of the DM halo itself barely contributes to the total binding energy of our system. Rather, the potential energy that binds the DM to the central BH outweighs all else.

Subsequently, to a good approximation, our binding energy goes as

$$U(r) = -\frac{4\pi G m_1 (R_{\rm core}^{2-\gamma_{\rm sp}} - r^{2-\gamma_{\rm sp}}) R_{\rm sp}^{\gamma_{\rm sp}} \rho_{\rm R}}{\gamma_{\rm sp} - 2}. \tag{3.9}$$

[iv] Electro-weak scale WIMP and standard MW values for normalization, mass of Sgr A*, etc.

3.1.3 Dynamical Friction Effects

Meanwhile, dynamical friction losses taken from Eq. (2.11) show that

$$\frac{\mathrm{d}E_{\mathrm{DF}}}{\mathrm{d}t} = 4\pi(Gm_2)^2\rho_{\mathrm{DM}}(r_2)\sqrt{\frac{m_1}{m_2}}v^{-1}, \tag{3.10}$$

where $\xi(v)$ has been excluded given that it is an $\mathcal{O}(1)$ term.

In the case that r_2 is static (i.e. the binary separation changes are irrelevant over the gigayear timescales we're exploring), we can simply perform separation of variables on this power loss equation to obtain the change in energy associated with dynamical friction effects:

$$\frac{\mathrm{d}E_{\mathrm{DF}}}{\mathrm{d}t} = 4\pi(Gm_2)^2\rho_{\mathrm{DM}}(r_2)\sqrt{\frac{m_1}{m_2}}v^{-1} \tag{3.11}$$

$$\mathrm{d}E_{\mathrm{DF}} = \mathrm{d}t \cdot 4\pi(Gm_2)^2\rho_{\mathrm{DM}}(r_2)\sqrt{\frac{m_1}{m_2}}v^{-1} \tag{3.12}$$

$$\Rightarrow \Delta E_{\mathrm{DF}} = t_{BH} \cdot 4\pi(Gm_2)^2\rho_{\mathrm{DM}}(r_2)\sqrt{\frac{m_1}{m_2}}v^{-1}. \tag{3.13}$$

In this simplified, linear regime, we now have an integrated, straightforward solution for our dynamical friction force.

3.1.4 Scouring Radius Calculation

Alright, now that we have a handle on both the dynamical friction and binding energy of our setup, one can take Eq. (3.1) to explicitly find an analytic expression

for the scouring radius $r_{\rm sc}$.

Again, for our power law profile, we solve for the radius at which the binary's loss in energy becomes comparable to the binding energy of the system itself. In other words, we set the aforementioned $U(r)$ to $\Delta E_{\rm DF}$ and solve for r:

$$\begin{aligned} r_{\rm sc} &\rightarrow U(r) = \Delta E_{\rm DF} \\ r_{\rm sc} &\rightarrow -\frac{4\pi G m_1 (R_{\rm core}^{2-\gamma_{\rm sp}} - r^{2-\gamma_{\rm sp}}) R_{\rm sp}^{\gamma_{\rm sp}} \rho_{\rm R}}{\gamma_{\rm sp} - 2} = \Delta E_{\rm DF}. \end{aligned} \tag{3.14}$$

Doing so, still under previous assumptions[v], yields the following:

$$r_{\rm sc} = \left(R_{\rm core}^{2-\gamma_{\rm sp}} + \frac{R_{\rm sp}^{-\gamma_{\rm sp}} (-2+\gamma_{\rm sp}) \Delta E_{\rm DF}}{4 G m_1 \pi \rho_{\rm R}} \right)^{\frac{1}{2-\gamma_{\rm sp}}}, \tag{3.15}$$

where $\Delta E_{\rm DF}$ is given by the derived expression in Eq. (3.13).

3.1.5 Modified Profile Definition

All the pieces are in place for our static spike case study, all we have left to do is fit the density profiles together in a physically meaningful way. Let's revisit the second assumption we've made in Sec. 3. We will still opt to neglect the intricate

[v] The self-interaction potential of the DM halo is negligible (1), and the companion BH's mass is sufficiently small such that $m_2 << m_1$ (2).

response of the halo to the injected energy until numerical approaches are feasible as a sanity check (see Sec. 4). Supposing that the center halo completely hallows out, we are now in position to define $\rho_{\rm mod}$, our final, binary-inclusive DM density profile

$$\rho_{\rm mod}(r) = \begin{cases} 0 & r \leq r_{\rm sc}, \\ \\ \rho_{\rm sp}(r) & r > r_{\rm sc}, \end{cases} \tag{3.16}$$

more explicitly written as

$$\Rightarrow \rho_{\rm mod}(r) = \begin{cases} 0 & r \leq \left(R_{\rm core}^{2-\gamma_{\rm sp}} + \frac{R_{\rm sp}^{-\gamma_{\rm sp}}(-2+\gamma_{\rm sp})\Delta E_{\rm DF}}{4Gm_1\pi\rho_{\rm R}} \right)^{\frac{1}{2-\gamma_{\rm sp}}}, \\ \\ \frac{\rho_{\rm R}\left(\frac{R_{\rm sp}}{r}\right)^{\gamma_{\rm sp}}\cdot\rho_{\rm core}}{\rho_{\rm R}\left(\frac{R_{\rm sp}}{r}\right)^{\gamma_{\rm sp}}+\rho_{\rm core}} & r > \left(R_{\rm core}^{2-\gamma_{\rm sp}} + \frac{R_{\rm sp}^{-\gamma_{\rm sp}}(-2+\gamma_{\rm sp})\Delta E_{\rm DF}}{4Gm_1\pi\rho_{\rm R}} \right)^{\frac{1}{2-\gamma_{\rm sp}}}. \end{cases} \tag{3.17}$$

Every variable above has been defined in previous chapters. We now have the capability of analyzing differences between the classic, single BH assumption and the proposed companion BH framework for the case of a static, cuspy initial profile.

3.2 Time Evolution & Spike Solution

However, before any further detailed analysis, it is informative to inquire about removing the first mathematical assumption we had made. In this section, we shall allow the binary separation, r_2, to significantly vary with time.

3.2.1 Energy versus Binary Separation

Let's begin by finding the change in energy associated with falling from r_0 in to some lower binary separation orbit, r_2:

$$\Delta E = \left(-\frac{Gm_1m_2}{r_2} - \left(-\frac{Gm_1m_2}{r_0}\right)\right) \tag{3.18}$$

$$= Gm_1m_2\left(\frac{1}{r_0} - \frac{1}{r_2}\right). \tag{3.19}$$

Solving for r_2 in terms of the change in energy ΔE associated with the binary system,

$$r_2 = \frac{Gm_1m_2r_0}{Gm_1m_2 - r_0\Delta E}. \tag{3.20}$$

The binary separation is now a function of the change of energy, which itself is a function of time, $r_2(\Delta E(t))$.

3.2.2 Time Promotion of Density

Given some density profile $\rho_0(r)$, we promote to a time-dependent profile $\rho(t, r)$ via energy dependence $\rho(\Delta E, r)$ as follows:

$$\rho(\Delta E, r) = \begin{cases} 0 & r \leq r_{sc}, \\ \\ \rho_0(r) & r > r_{sc}. \end{cases} \tag{3.21}$$

For our power law profile, we solve for the radius at which the binary's loss in energy becomes comparable to the binding energy of the system itself, once again. This recovers the static result earlier expressed in Eq. (3.15).

3.2.3 Time Evolution of Energy Loss

Re-expressing the dynamical friction loss in terms of our new, $\rho(\Delta E, r)$ and time-dependent r_2:

$$\frac{\mathrm{d}E_{\mathrm{DF}}}{\mathrm{d}t} = P\left[r_2(\Delta E)\,, \rho\left(\Delta E, r_2(\Delta E)\right)\right]. \tag{3.22}$$

Now, notice that

$$\frac{\mathrm{d}E_{\mathrm{DF}}}{\mathrm{d}t} = \frac{\mathrm{d}\Delta E_{\mathrm{DF}}}{\mathrm{d}t}. \tag{3.23}$$

So, we can separate the differential equation as

$$\mathrm{d}t = -\frac{1}{P\left[r_2(\Delta E)\,, \rho\left(\Delta E, r_2(\Delta E)\right]\right.}\,\mathrm{d}\Delta E, \tag{3.24}$$

and thereby obtain

$$t(\Delta E) = \int_0^{\Delta E} \frac{-1}{P(\delta E)}\,\mathrm{d}\delta. \tag{3.25}$$

This is fantastic, now we have a complete framework to follow and calculate the time evolution of our hidden friend system! Simply casting everything in terms of the energy transfer is sufficient to create $P(\Delta E)$ the power associated with dynamical friction losses.

We've obtained the official binding energy of the BH binary system with a DM halo, took the density to be a piecewise with its cutoff at $r_{\rm sc}$, as well promoted any previous time ambiguities to functions of $\Delta E(t)$.

3.2.4 Altogether, for a Power Law

An important note: in this simple model, we are removing all of the DM from the center. Thus, the dynamical friction eventually falls to zero when the coring radius exceeds the binary separation. This gives rise to a maximum energy loss, below called $\Delta E_{\rm bound}$. This is not exact, but it should be a reasonable approximation to retaining the halo core.

Ultimately, what we wish to obtain is a value for the binary separation $r_2(\Delta E)$ after our system relaxes to below our energy loss bound, $\Delta E_{\rm bound}$.

To calculate $\Delta E_{\rm bound}$, we inspect the magnitude of energy loss at which the scouring radius $r_{\rm sc}$ overtakes the initial binary separation r_2:

$$\Delta E_{\rm bound} \to r_{\rm sc}(\Delta E) = r_2(\Delta E). \tag{3.26}$$

Once found, one can set a relevant time-scale of interest[vi]. We now take Eq. (3.25) and ask: for what value of δE does $t(\Delta E)$ become equal to a gigayear?

In our Mathematica coding journey, we initialize our find root algorithm to search nearest to ΔE_{bound}. This will immediately yield some energy value δE_{Gyr} associated with our 1 Gyr time. Then, immediately plugging this value back into the calculation for $r_2(\Delta E)$, this time as $r_2(\delta E_{\text{Gyr}})$, we quantitatively discover what value the binary separation should fall into, given the hidden friend system evolves over some timescale!

In turn, this is all we really need to define a final density profile ρ_{mod}, dependent on the time-evolved binary separation.

As an example, consider $t_{\text{BH}} = 1$ Gyr, $m_1 = 10^6$ $\text{M}_\odot$, $m_2 = 10^0$ $\text{M}_\odot$, normalization $r_0 = 1$ au, $\rho_0 \approx 224$ $\text{M}_\odot/\text{pc}^3$ and $\gamma = 1.75$. For the sake of simplicity, we'll define our generic WIMP to be of electro-weak scale mass: $m_\chi = 100$ GeV, with an annihilation cross-section $\sigma v = 10^{-26}$ cm^3/s. We initialize our system to have an initial companion separation of 10^3 au. In this case, we produce Fig. 3.2, tracking the evolution of the fractional change in binary separation.

While we cannot generalize for the entire parameter space, we see that this instance does have significant changes to the binary separation over t_{BH}.

[vi] As before, we will consider evolving the system over the range of roughly 1 Gyr.

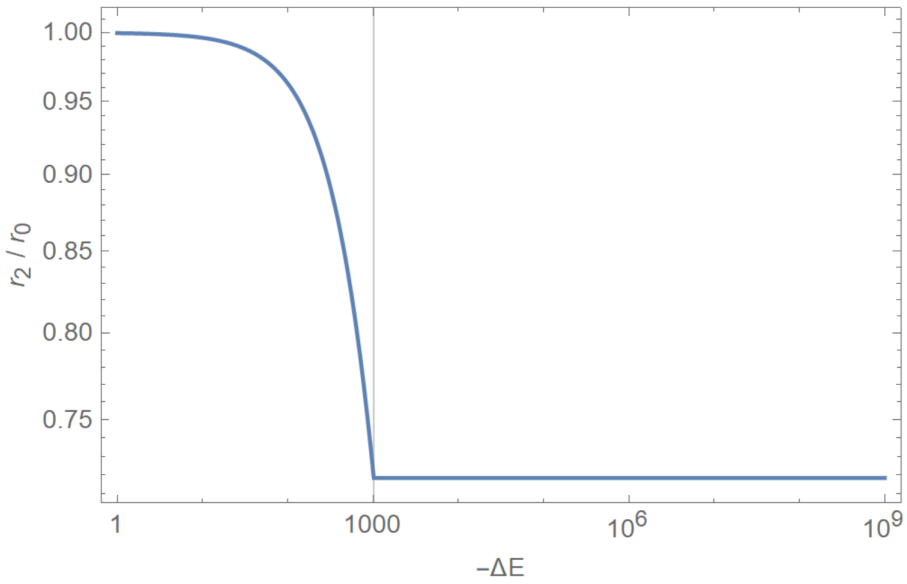

Figure 3.2: Mathematica plot illustrating time evolved BH binary system with surrounding DM halo. r_2/r_0, the evolved versus intial binary separation are plotted against the change in energy of the binary system, ΔE. The light vertical line shows where ΔE_{bound} is for this particular setup.

4

Numerical Sanity Check

We are able to catch a glimpse into just how robust our second assumption (the halo's dynamic response to injected energy) is, thanks to code for computing the time evolution and properties of the DM spike, publicly available online at `https://github.com/bradkav/HaloFeedback` [17].

Under the condition that we keep the orbital separation *fixed*[i], we may look at how the DM spike evolves in response to energy injection. We consider a mass $m_2 = 10^3\ \mathrm{M}_\odot$ orbiting a central BH $m_1 = 10^6\ \mathrm{M}_\odot$ at a distance $r_2 = 10^8$ pc. This is a typical set of parameters associated with the "allowable" regime in our parameter space [12]. Evolving this system over roughly 0.1 Gyr[ii] and with 10^3 orbits per computational step, we find significant scouring effects near the fixed, binary separation radius. We

[i] The orbit of the compact object cannot change.

[ii] Equivalent to 10^7 orbits, $\approx 4 \times 10^9$ days.

must take these results with a grain of salt, given that our fractional error in energy conservation approached 33%.

Further computation, comparison, and analysis will be necessary. In the near future, we plan to increase simulation resolution and number of orbits to get a clearer picture of our binary's dynamics. Furthermore, it is known that the amount of dynamical friction effects will rapidly fall off as we deplete the DM content directly surrounding the binary system. Ideally, we can remove the assumption that r_2 is fixed and clarify details as to the evolution of these types of binary configurations.

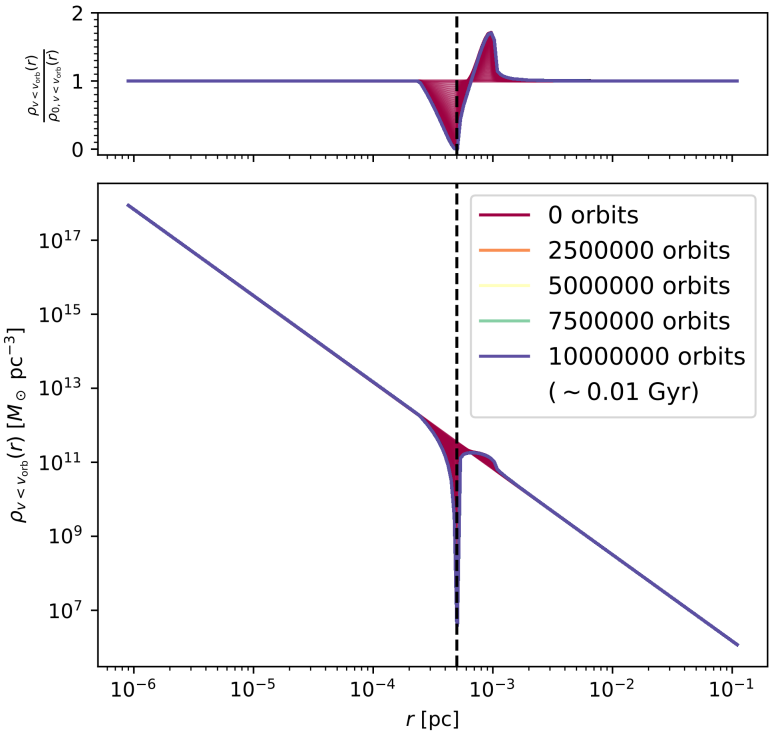

Figure 4.1: Evolution of the DM spike density profile for a typical Milky Way binary case, due to feedback from the orbiting companion (over 0.01 Gyr). We consider $m_1 = 10^6$ $M_\odot$, $m_2 = 10^3$ $M_\odot$, orbiting at a fixed radius of $r_2 = 10^8$ pc. Note that we plot $\rho_{\rm DM}(r)$ multiplied by the fraction of DM at some radius r moving slower than the local orbital speed $v_{\rm orb}(r)$. Simulation and plots created from [17].

5

Generalization of DM Spike

All previous work conducted was under the expectation that we have an initial cuspy, single power law DM profile: this is not necessarily the case. In fact, a more well-known spatial mass profile often used in the DM industry is the Navarro-Frenk-White (NFW) profile [18].

5.1 Navarro-Frenk-White (NFW) profile

This is, in essence, a broken power law fit to a given DM halo:

$$\rho_{\mathrm{NFW}}(r) = \frac{\rho_0}{\frac{r}{r_0}\left(1+\frac{r}{r_0}\right)^2}. \tag{5.1}$$

To get a better handle on the physics of our hidden friend configuration, we should

also better understand different shapes of initial profiles!

We argue that that the DM distribution at our galactic center, if not a spike, is represented by some generalized NFW profile. In the limit $r \to 0$, our density will appear to be a power law with some inner index or slope parameter[i]. Since the dynamics of host-companion-DM interaction we care about are localized to small radii compared to the NFW scale radius, we can neglect the broken power law nature of an NFW system and instead approach it as a simple power law problem.

Here, we take the ρ_{NFW} profile and series expand for simplicity, neglecting higher order terms other than the leading $\mathcal{O}(1/r)$:

$$\rho_{\text{NFW}}(r) \approx \frac{r_0 \rho_0}{r} + \mathcal{O}(r^0). \tag{5.2}$$

This problem has now been reduced to a generic power law, with an associated slope parameter $\gamma = 1$. For the Milky Way, our galactic system of interest, these normalizations take on specific values via observation: the Milky Way has a scale radius of roughly 16.1 kpc along with a scale density of 1.4×10^7 $\text{M}_\odot/\text{kpc}^3$. For both the static and time-evolved case, the arguments and derivations from Sec. 3.1 and Sec. 3.2 still apply.

[i] For an NFW profile (not generalized), this inner power index is 1.

6

Impacts of Companion

6.1 J-Factor Analysis

By simply identifying a dark matter structure and a particle dark matter model, we can make estimates for prompt emission, which produces photons in the gamma-ray energy range for WIMPs [19]. For concreteness, we will consider dark matter annihilation events rather than any other form of interaction.

We ask, what are the optimal targets and expected detection rates for these DM annihilation searches? Well, the flux of photons produced by DM annihilation from a given direction ψ in the sky and from within some solid angle $\Delta\Omega$ is

$$\phi_\gamma = \frac{\Delta\Omega}{4\pi}\left\{\frac{1}{\Delta\Omega}\int \mathrm{d}\Omega \int \mathrm{d}l(\psi)(\rho_{\mathrm{DM}})^2\right\}\frac{\langle\sigma v\rangle}{2m_\chi^2}\frac{\mathrm{d}N_\gamma}{\mathrm{d}E_\gamma}, \tag{6.1}$$

where this mysterious, last factor is a sum of the prompt gamma-ray spectrum from every possible annihilation final state f:

$$\frac{\mathrm{d}N_\gamma}{\mathrm{d}E_\gamma} = \sum_f \frac{\mathrm{d}N_\gamma^f}{\mathrm{d}E_\gamma}. \tag{6.2}$$

Most pertinent to our exploration is the term in curly brackets, often referred to as the "J-factor." This function of solid angle $\Delta\Omega$ and the direction in the sky, $J = J(\Delta\Omega, \psi)$, carries units of $\mathrm{GeV}^2/\mathrm{cm}^5$. Realistically, the solid angle $\Delta\Omega$ should be optimized for a given detector and target, field of view and angular resolution to maximize the signal-to-noise ratio [19].

J-factors are terms which describe the distribution of DM in a given astrophysical system, determining the strength of the signal provided by annihilating or decaying DM. Notice that the J-factor is directly proportional to the photon flux of self-annihilating DM particles: in understanding the J-factors for a given dark matter distribution and particle model, we can better understand the expected production rates of gamma-ray photons, for example.

Through a comparison of the luminosities produced by our initial and evolved profiles, we compare ρ_{sp} with our newly made, binary inclusive profile, ρ_{mod}. We can now calculate the quantitative effect of a companion on the surrounding DM by using these J-factors. Here's what that looks like, roughly:

$$J(\Delta\Omega, \psi) \approx \int \mathbf{dl}(\psi)(\rho_{\mathrm{DM}})^2. \tag{6.3}$$

This represents an integral over our line-of-sight, where density changes towards the center are important due to our factor of ρ_{DM}^2.

Finally, let's plot the attenuation of DM annihilation signals as we've calculated above. Again, the x-axis will represent the companion BH's solar mass, and the y-axis, the binary separation of our hidden friend system. The purplish shaded regions represent the most stringent constraints set by the Naoz et al. paper [12], making the bounded center piece physically allowable. The color axis, the ratio of "mod-to-sp" J-factors, ranges from 10^0, no change, to 10^{-8}:

Indeed! The annihilation luminosity is attenuated by a significant factor, even in a conservative case. Comparing the allowable regime on our plot to the color axis, we see a minimum of $\mathcal{O}(10^0)$ changes to a maximum of some $\mathcal{O}(10^4)$ that are possible! We've set γ, our slope parameter to 1.75, the annihilation cross section along with DM mass to a typical electro-weak model value ($\sim$ 100 GeV), and the angle of observation for the line-of-sight integral to a single degree. Even in the case that we set $\gamma = 1$, we still see order of magnitude changes to what we'd normally expect.

For a majority of the physically allowed parameter space, significant scouring effects lead to a decrease in expected luminosity signals from the center of our Milky Way system! This could potentially remove DM annihilation as an explanation of

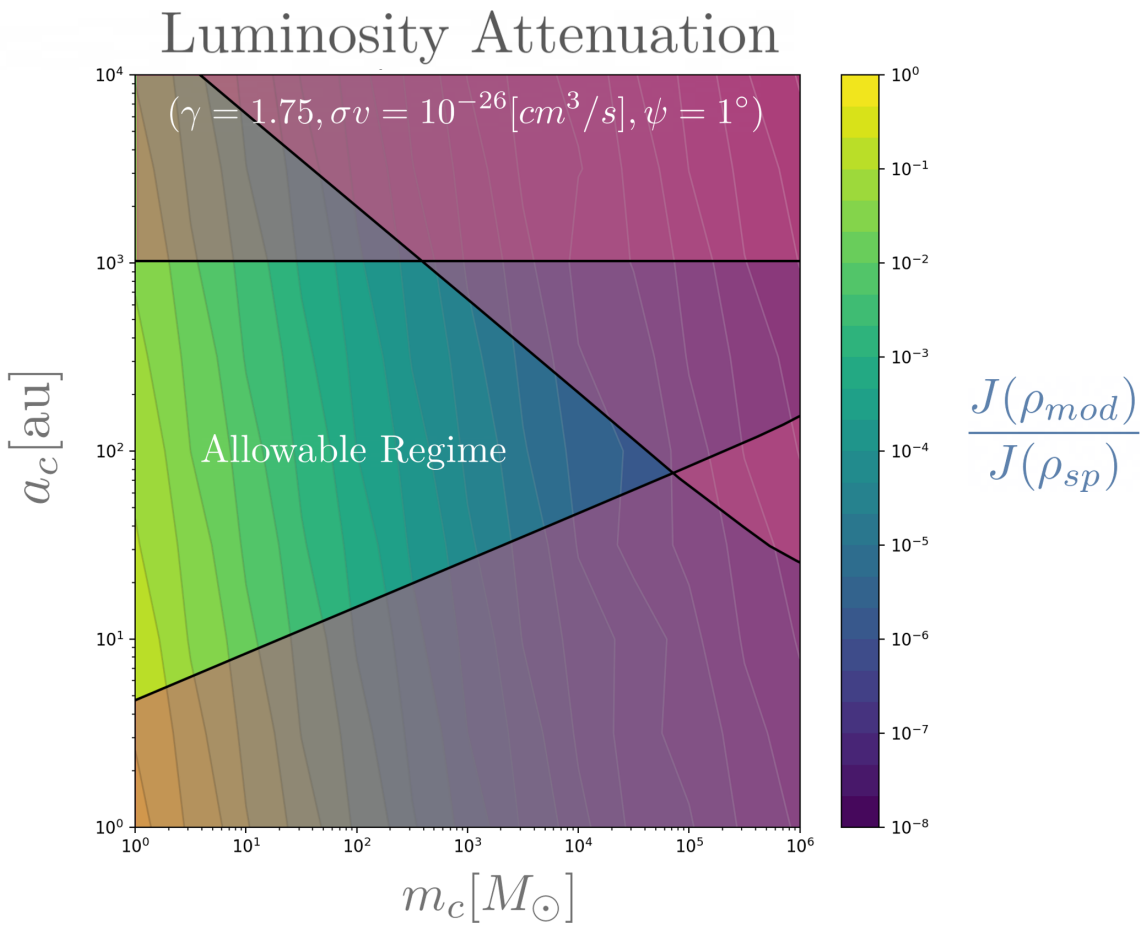

Figure 6.1: Attenuation of luminosity via J-factor ratio. Illustrates the expected change in signal strength assuming various initial parameters for Sgr A* Hidden Friend system.

our galactic center excess and revolutionize the models seen as effective in treating the mystery of DM. If such a binary is discovered in the near future, there will be significant implications for DM annihilation bounds as well as the interpretation of aforementioned gamma-ray, galactic center excess.

7

Conclusion

There are many interesting prospects for the existence and detection of a companion BH in our Milky Way, and we have explicitly estimated the impact of such an object on any DM spike that might have formed in our galaxy.

The existence of such a binary system has immense consequences for the distribution of DM at the galactic center. Consequently, as DM begins to crowd together and collide in this highly-dense region of space, there are dramatic implications for the DM annihilation signals that we detect from Earth's comfort.

Through our theoretical framework, we have shown that dark matter annihilation's claimed relevance to the galactic center excess[i] can be substantially weakened by the presence of a binary BH system at the center of our Milky Way. By relaxing these

[i] An overabundance of high energy gamma rays originating from the galactic center

constraints with the consideration of a companion black hole, we completely open up the door to previously eliminated bands of dark matter candidates, revitalizing our search focus and providing further fodder for future dark matter exploration.

This inquiry presented will cast light upon the elusive mysteries of DM and its detection, the dynamics of the most extreme entities in existence, along with their combined interplay.

We are on a journey to make the invisible visible.

8

Bibliography

[1] P. Ullio, H. Zhao and M. Kamionkowski, *A Dark matter spike at the galactic center?*, *Phys. Rev. D* **64** (2001) 043504, [astro-ph/0101481].

[2] A. M. Ghez, B. L. Klein, M. Morris and E. E. Becklin, *High proper motion stars in the vicinity of Sgr A*: Evidence for a supermassive black hole at the center of our galaxy*, *Astrophys. J.* **509** (1998) 678–686, [astro-ph/9807210].

[3] J. M. Lotz, P. Jonsson, T. J. Cox, D. Croton, J. R. Primack, R. S. Somerville et al., *The Major and Minor Galaxy Merger Rates at $z < 1.5$*, *Astrophys. J.* **742** (2011) 103, [1108.2508].

[4] L. Goodenough and D. Hooper, *Possible Evidence For Dark Matter Annihilation In The Inner Milky Way From The Fermi Gamma Ray Space Telescope*, 0910.2998.

[5] A. Medeiros Da Rosa, *Adiabatic Dark Matter Density Cusps Around*

Supermassive Black Holes and Dark Matter Detection, Ph.D. thesis, Washington U., St. Louis, 2019. 10.7936/205a-j912.

[6] G. D. Quinlan, L. Hernquist and S. Sigurdsson, *Models of Galaxies with Central Black Holes: Adiabatic Growth in Spherical Galaxies*, *Astrophys. J.* **440** (1995) 554–564, [astro-ph/9407005].

[7] D. Merritt, M. Milosavljevic, L. Verde and R. Jimenez, *Dark matter spikes and annihilation radiation from the galactic center*, *Phys. Rev. Lett.* **88** (2002) 191301, [astro-ph/0201376].

[8] G. Bertone and D. Merritt, *Time-dependent models for dark matter at the Galactic Center*, *Phys. Rev. D* **72** (2005) 103502, [astro-ph/0501555].

[9] J. Kormendy and D. Richstone, *Inward bound: The Search for supermassive black holes in galactic nuclei*, *Ann. Rev. Astron. Astrophys.* **33** (1995) 581.

[10] J. M. D. Kruijssen, J. L. Pfeffer, M. Reina-Campos, R. A. Crain and N. Bastian, *The formation and assembly history of the Milky Way revealed by its globular cluster population*, **486** (July, 2019) 3180–3202, [1806.05680].

[11] M. Unavane, R. F. G. Wyse and G. F. Gilmore, *The merging history of the milky way*, *Mon. Not. Roy. Astron. Soc.* **278** (1996) 727–736, [astro-ph/9509030].

[12] S. Naoz, C. M. Will, E. Ramirez-Ruiz, A. Hees, A. M. Ghez and T. Do, *A*

*hidden friend for the galactic center black hole, Sgr A**, *Astrophys. J. Lett.* **888** (2020) L8, [1912.04910].

[13] D. H. Weinberg, J. S. Bullock, F. Governato, R. Kuzio de Naray and A. H. G. Peter, *Cold dark matter: controversies on small scales*, *Proc. Nat. Acad. Sci.* **112** (2015) 12249–12255, [1306.0913].

[14] M. Rocha, A. H. G. Peter, J. S. Bullock, M. Kaplinghat, S. Garrison-Kimmel, J. Onorbe et al., *Cosmological Simulations with Self-Interacting Dark Matter I: Constant Density Cores and Substructure*, *Mon. Not. Roy. Astron. Soc.* **430** (2013) 81–104, [1208.3025].

[15] J. M. Cline, G. Gambini, S. D. Mcdermott and M. Puel, *Late-Time Dark Matter Oscillations and the Core-Cusp Problem*, *JHEP* **04** (2021) 223, [2010.12583].

[16] P. Gondolo and J. Silk, *Dark matter annihilation at the galactic center*, *Phys. Rev. Lett.* **83** (1999) 1719–1722, [astro-ph/9906391].

[17] B. J. Kavanagh, D. A. Nichols, G. Bertone and D. Gaggero, *Detecting dark matter around black holes with gravitational waves: Effects of dark-matter dynamics on the gravitational waveform*, *Phys. Rev. D* **102** (2020) 083006, [2002.12811].

[18] J. F. Navarro, C. S. Frenk and S. D. M. White, *The Structure of cold dark matter halos*, *Astrophys. J.* **462** (1996) 563–575, [astro-ph/9508025].

[19] S. Profumo, L. Giani and O. F. Piattella, *An Introduction to Particle Dark Matter*, *Universe* **5** (2019) 213, [1910.05610].